forum acusticum 2026
8-12 September · Graz, Austria

Pressure field calculation using the Born series method for an array of point sources in inhomogeneous fractional viscoacoustic medium

Ujjal Mandal[1], Jagpreet Singh[2], Ben T Cox[3], Ratan K Saha[1]

[1] *Department of Applied Sciences, Indian Institute of Information Technology Allahabad, Jhalwa, Prayagraj 211015, Uttar Pradesh, India*

[2] *Department of Computer Science and Engineering, Indian Institute of Technology Ropar, Street 29, Ropar, 140001, Punjab, India*

[3] *Department of Medical Physics and Biomedical Engineering, University College London, Gower Street, London, WC1E 6BT, UK*

This paper is a revised version of the authors' submitted manuscript that was peer-reviewed by at least two anonymous reviewers.

Abstract

Steady-state pressure field simulation, for a ultrasound transducer owing to time harmonic excitation, remains an active area of research because it provides important information regarding beam profile along the axial and lateral directions, and its convergence at the focal region and modification in the field due to scatterers etc. In this work, traditional Born series (TBS) approach has been applied to calculate the pressure field for a linear array of point sources. A total of 501 points was considered. The simulation was performed in a square computational domain of size 4096×4096 grid points with spatial resolution of 20 μm and the medium was considered to be absorbing, dispersive and inhomogeneous. The numerical code was written in CUDA C and was executed in a GPU architecture. The estimated field at ≈ 1 MHz demonstrates excellent agreement with that of a standard time-domain method. This study reveals that the TBS procedure has the potential for rapid computation of pressure fields for real transducers.

Keywords: *Tine-harmonic excitation, k-Wave, GPU, absorbing-dispersive medium, inhomogeous medium*

1. Introduction

Ultrasound imaging is an essential tool in modern healthcare. It helps in making a clinical decision without exposing the patient to risk [1]. The growing use of non-invasive diagnostic methods has increased the adoption of ultrasound in clinical practice. While conventional B-mode ultrasound is widely used, it has limitations in resolution and tissue characterization. Advanced techniques such as ultrasound computed tomography (USCT) improve imaging by reconstructing quantitative tissue properties using the full waveform inversion method [2], [3]. However, these approaches require accurate and computationally intensive modeling of wave propagation in complex biological tissues. Recent advances in transcranial US treatments including blood brain barrier modulation for drug delivery highlight the importance of wave propagation [4]. Wave propagation is also essential for probe design and algorithm development in US systems.

Accurate modeling of wave absorption and dispersion in lossy media is essential in medical ultrasound imaging. It has been experimentally shown that acoustic absorption in biological tissue follows a frequency power law of the form $\alpha = \alpha_0 \omega^\nu$, where α_0 is the attenuation coefficient, ν is the power law exponent, ω as the angular frequency of the wave [5]. The typical numerical values of these parameters for biological tissue are 5.5×10^{-10} Np (rad/s)$^{-\nu}$ m^{-1} and $\nu = 1.5$, respectively.

Earlier constitutive models relied on temporal fractional derivatives for describing power-law absorption. These operators are inherently non-local in time, requiring access to the full time history of the field variables during numerical implementation and create high computational demands [6]. Treeby et al., efficiently solved this problem (without the need to store the time history) and thus significantly reduced the memory requirement [7]. In this work, we apply the traditional Born series (TBS) method to solve inhomogeneous Helmholtz equation. The classical Born series (BS) method was developed by Max Born while studying scattering problems in quantum mechanics and it is referred to as the TBS in this study [8]. Recently, Osnabrugge et. al, [9] developed a modified version of the TBS technique, which is termed as the

Corresponding author: *ratank.saha@iiita.ac.in.*

convergent Born series (CBS) in the literature. This approach employs a preconditioning strategy to ensure convergence for strongly scattering media, however, the TBS is generally applicable to weak scattering regimes [10], [11], [12], [13]. The pressure field at $\approx$ 1 MHz has been calculated in an absorbing, dispersive and heterogeneous medium generated by a linear array of point sources utilizing the TBS framework. A CUDA C code developed for this purpose was executed in a GPU machine. It provided the desired result very rapidly. The TBS method seems to be a promising candidate for large scale simulations.

2. Background

2.1. Absorbing and dispersive medium

The time dependent wave equation for an absorbing and dispersive but otherwise homogeneous medium in terms of fractional derivatives can be written as [7],

$$\{\nabla^2 - \tfrac{1}{v_f^2}\partial_t^2 + \tau\partial_t(-\nabla^2)^{\frac{\nu}{2}} + \eta(-\nabla^2)^{\frac{\nu+1}{2}}\}p(\mathbf{r},t) = 0, \quad (1)$$

where v_f is the speed of sound for the wave propagating medium; two proportionality constants are expressed as, $\tau = -2\alpha_0 v_f^{\nu-1}$, $\eta = 2\alpha_0 v_f^{\nu}\tan(\frac{\pi\nu}{2})$; The time-independent wave equation would be [13],

$$\nabla^2\tilde{p}(\mathbf{r}) + k_f^2\tilde{p}(\mathbf{r}) = V_1(\mathbf{r})\tilde{p}(\mathbf{r}), \quad (2)$$

where,

$$V_1(\mathbf{r}) = \{i\tau\omega(-\nabla^2)^{\frac{\nu}{2}} - \eta(-\nabla^2)^{\frac{\nu+1}{2}}\}, \quad (3)$$

with k_f is the wavenumber for the medium. The terms on the right hand side of Eq. (3) are responsible for attenuation and dispersion of the wave, respectively. Further, these terms individually or jointly can be thought of as a potential term as seen from Eq. (2).

2.2. Scattering medium

Consider a region whose acoustic impedance is slightly different than the surrounding medium. For such a heterogeneous medium, the time-dependent wave equation becomes,

$$\{\nabla^2 - \frac{1}{v_f^2}\partial_t^2\}p(\mathbf{r},t) = \gamma_\kappa(\mathbf{r},t)\partial_t^2 p(\mathbf{r},t) + \nabla\cdot[\gamma_\rho(\mathbf{r},t)\nabla p(\mathbf{r},t)], \quad (4)$$

with $\gamma_\kappa(\mathbf{r},t) = \{\kappa_s(\mathbf{r},t) - \kappa_f\}/\kappa_f$ and $\gamma_\rho(\mathbf{r},t) = \{\rho_s(\mathbf{r},t) - \rho_f\}/\rho_s(\mathbf{r},t)$ inside the scatterer and $\gamma_\kappa(\mathbf{r},t) = \gamma_\rho(\mathbf{r},t) = 0$ outside the scatterer; ρ and κ are the density and compressibility of the medium, respectively; the subscripts s and f state the source and the ambient fluid medium, respectively. And for $\rho_s \approx \rho_f$, the time-independent wave equation reduces to,

$$\nabla^2\tilde{p}(\mathbf{r}) + k_f^2\tilde{p}(\mathbf{r}) = V_2(\mathbf{r})\tilde{p}(\mathbf{r}), \quad (5)$$

where,

$$V_2(\mathbf{r}) = \begin{cases} -(k_s^2 - k_f^2), & \text{inside the scatterer} \\ 0. & \text{outside the scatterer} \end{cases} \quad (6)$$

Here, k_s is the wavenumber of the scattering region.

2.3. Born series formulation

The general form of the inhomogeneous Helmholtz equation in the presence of an active acoustic source and scattering inhomogeneity can be cast as [9],

$$\nabla^2\tilde{p}(\mathbf{r}) + (k_f^2 + i\epsilon)\tilde{p}(\mathbf{r}) = -S(\mathbf{r}) - V(\mathbf{r})\tilde{p}(\mathbf{r}), \quad (7)$$

where, $\epsilon \in \mathbb{R}^+$, which makes the entire medium attenuating and hence ensures convergence of the field [9]; $S(\mathbf{r})$ and $V(\mathbf{r})$ indicate the source and the scattering potential, respectively; for example, for an acoustically inhomogeneous region, $V(\mathbf{r})$ becomes, $V(\mathbf{r}) = k_s^2 - k_f^2 - i\epsilon$. The integral formulation of Eq. (7) yields [9], [14],

$$\tilde{p}(\mathbf{r}) = \int g(\mathbf{r} - \mathbf{r}_0)[V(\mathbf{r}_0)\tilde{p}(\mathbf{r}_0) + S(\mathbf{r}_0)]d^2\mathbf{r}_0. \quad (8)$$

for a 2D system and $g(\mathbf{r} - \mathbf{r}_0)$ is the Green's function satisfying,

$$\{\nabla^2 + (k_f^2 + i\epsilon)\}g(\mathbf{r} - \mathbf{r}_0) = -\delta(\mathbf{r} - \mathbf{r}_0). \quad (9)$$

Here, $\delta(\mathbf{r} - \mathbf{r}_0)$ is the Dirac delta function. Since Eq. (8) contains convolution operations, it can be rewritten as,

$$\tilde{p} = GV\tilde{p} + GS. \quad (10)$$

where G is an operator and is defined as, $G = \text{IFFT}\tilde{g}(\mathbf{K})\text{FFT}$; FFT and IFFT represent the forward and inverse Fourier transform operators, respectively; $\tilde{g}(\mathbf{K})$ is a frequency domain function and is given by, $\tilde{g}(\mathbf{K}) = \frac{1}{(|\mathbf{K}|^2 - k_f^2 - i\epsilon)}$, $\mathbf{K}$ is the Fourier transformed coordinates. After rearranging terms in Eq. (10) and the standard binomial expansion of $(1 - GV)^{-1}$ provides,

$$\tilde{p} = \sum_{n=0}^{\infty}(GV)^n GS. \quad (11)$$

Eq. (11) is the famous traditional Born series (called the Born series). The series converges when spectral norm of $|GV| < 1$ is satisfied [15].

2.4. Numerical implementation

Using the linear superposition principle and utilizing Eqs. (2) and (5), the Helmholtz equation for an inhomogeneous-absorbing-dispersive medium can be presented as,

$$\nabla^2\tilde{p}(\mathbf{r}) + (k_f^2 + i\epsilon)\tilde{p}(\mathbf{r}) = -S(\mathbf{r}) - \{-i\tau\omega(-\nabla^2)^{\nu/2} + \eta(-\nabla^2)^{(\nu+1)/2} + (k_s^2 - k_f^2 - i\epsilon)\}\tilde{p}(\mathbf{r}). \quad (12)$$

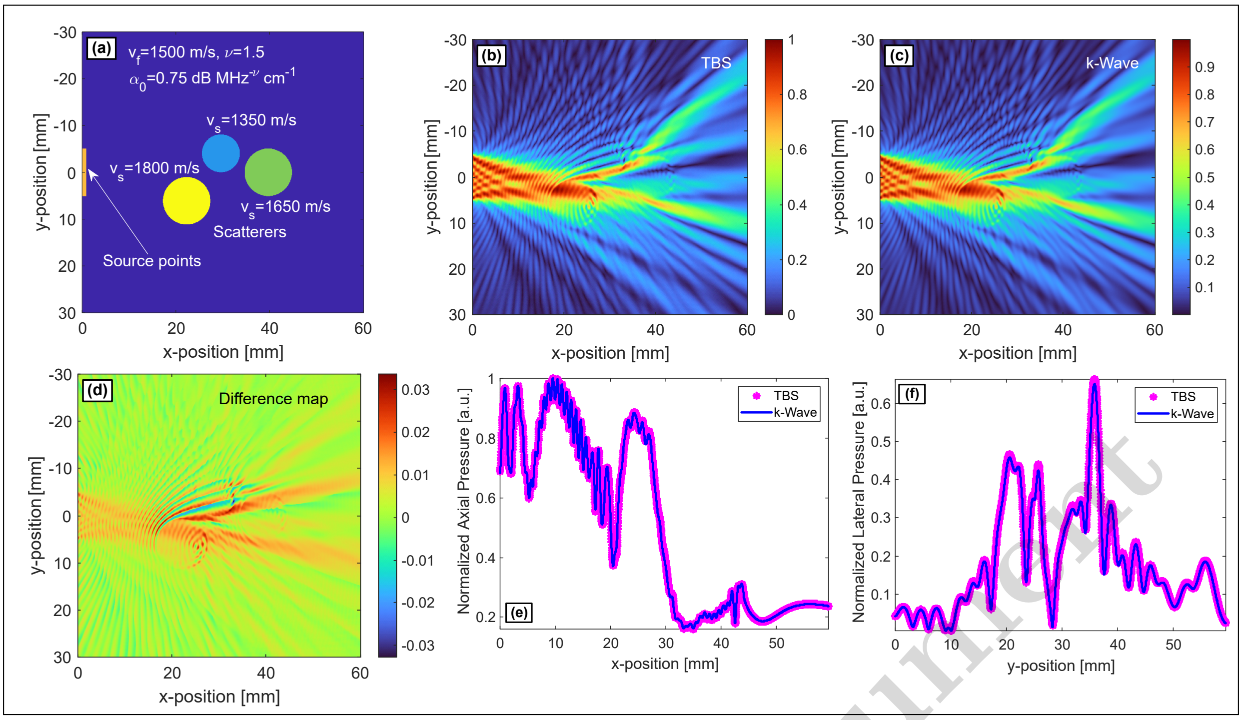

Figure 1: (a) Simulation arrangement for a complex medium (absorbing, dispersive and scattering) with a linear phased-array source and three scatterers with size-dispersity and strength-heterogeneity. (b) and (c) Spatial distributions of normalized pressure for the medium shown in (a) and generated using the TBS and k-Wave methods, respectively. (d) Error map (difference between the TBS and k-Wave results). (e) Steady state normalized pressure amplitude along the axis of the transducer. (f) Same as (e) but for a transverse line.

The field was initialized before the start of the iterative process,

$$\tilde{p}^0(\mathbf{r}) = \mathrm{IFFT}[\tilde{g}(\mathbf{K})\mathrm{FFT}[S(\mathbf{r})]]. \tag{13}$$

The pressure field at the $(l+1)^{th}$ iteration was updated using the following expression,

$$\tilde{p}^{l+1}(\mathbf{r}) = \mathrm{IFFT}[\tilde{g}(\mathbf{K})[\{-i\tau\omega k^{\nu} + \eta k^{\nu+1}\}\mathrm{FFT}[\tilde{p}^l(\mathbf{r})] + \mathrm{FFT}[U\tilde{p}^l(\mathbf{r}) + S(\mathbf{r})]]], \tag{14}$$

using the Fourier transform property of the fractional Laplacian, $\mathrm{FFT}[(-\nabla^2)^{\nu/2}\tilde{p}^l(\mathbf{r})] = k^{\nu}\mathrm{FFT}[\tilde{p}^l(\mathbf{r})]$ and defining, $U = k_s^2 - k_f^2 - i\epsilon$ within the scatterer else $-i\epsilon$.

3. Numerical experiment

The numerical simulation was performed in a computational domain of size 4096×4096 grid points with spatial resolution $dx = dy = 20$ μm. The background sound-speed and density were considered as, $v_f = 1500$ m/s and $\rho = 1000$ kg/m^3, respectively. For this numerical experiment, three scatterers of different sizes and contrasts were placed at distinct locations in the mixed medium as shown in Fig. 1(a). A linear array consisting of 501 point sources was placed at a distance $675dx$ from the left edge of the computational domain. The magnitude of $S(\mathbf{r})$ was set to $|S(m, 675)| = 10^6$ Pa/m^2 with $m \in [1799..2299]$. The acoustic pressure field was computed iteratively at a frequency $f = 1007.080$ kHz with $\epsilon = 0.8k_f^2$. This frequency is a harmonic of the fundamental frequency supported by the discretized computational domain.

During each iteration, the pressure field was multiplied by a matrix (designated as ABLMatrix) to minimize reflections from the boundaries [13], [15]. The absorbing property at each boundary of this matrix was enabled by constructing it using a sigmoid function, $ABLSig(x) = 1/(1 + \exp(-\zeta(x - 0.5\mu)))$ else unity was assigned to it. The tuning parameter was chosen as $\zeta = 21.48$ Np/cm and μ denotes the thickness of the absorbing layer. Therefore, when a field was multiplied by this matrix, the field values at the boundaries were attenuated significantly but those of the other locations remained unaltered.

Beam steering was also introduced in the transducer array. The iterative solution was considered to converge when the error was below the threshold value of $\mathrm{TErr} \leq 10^{-5}$. The error was evaluated along the center line of the computational domain as,

$$\mathrm{TErr} = \frac{\sum_{m=1}^{4096} |\tilde{p}_{l+1}(2049, m) - \tilde{p}_l(2049, m)|}{\sum_{m=1}^{4096} |\tilde{p}_l(2049, m)|}. \tag{15}$$

The results obtained by the TBS method were compared and validated by running the same simulations in the k-Wave toolbox [7]. The GPU code was written using CUDA C in order to implement Eq. (14)

and was executed on a workstation [13], [15]. The corresponding k-Wave data were also generated for comparison.

4. Numerical results and discussion

An interesting result is observed in this experiment. As the steered beam propagates from the linear array, it interacts with the scatterers located in its path, causing the main lobe of the beam to split due to scattering effects. The geometrical configuration of the computational domain (without the absorbing boundaries) is illustrated in Fig. 1(a). Normalized pressure distributions using two different procedures are shown in Figs. 1(b) and (c), respectively. The corresponding difference map is presented in Fig. 1(d), which shows a maximum discrepancy of approximately 3%, indicating a close agreement between the TBS and k-Wave results. The axial and lateral variations of the pressure field along the center line are drawn in Figs. 1(e) and (f). These figures exhibit perfect match of normalized results facilitated by the methods mentioned herein.

Note that all addition and multiplication operations in Eq. (14) were carried out element wise making the method very much suitable for implementation in GPU [13], [15]. The parameter ϵ makes the ambient medium attenuating and consequently, Green's function becomes lossy; also the total energy of the function becomes finite and localized. The propagation speed of the field with iteration grows as ϵ decreases resulting in faster convergence of the field. However, for the CBS method, ϵ cannot be arbitrarily chosen because it has to satisfy $\epsilon \geq \max|k_s^2 - k_f^2|$. As discussed earlier, $ABLSig$ matrix has been constructed and it contains specially designed absorbing layers at the boundaries. The entries of this matrix at the absorbing layers fall off at a very slow rate from unity, minimizing reflection of the wave. Moreover, its values reach to zero very gently at the edges of the computational domain warranting that the wave would not reappear from the opposite edge. These features of the absorbing layer of each side guarantee convergence of the field. As stated earlier, the TBS technique works faithfully for weak scatters. For example, it is shown that for a circular solid scatterer of radius a with 30% sound-speed mismatch, the TBS method provides converging results when $k_f a < 25$ whereas for -20% sound-speed mismatch, validity limit is $k_f a < 9$ [11]. The CBS results however do not diverge for such scatters [11].

The current study includes a single example at one frequency. This is particularly relevant in biomedical applications, where low frequencies (e.g., $\approx$ 1 MHz) are often used for neuromodulation [16]. Higher frequencies (e.g., 3–10 MHz) are more relevant for ultrasound imaging, which is accomplished using various transducers. A systematic investigation across multiple frequencies and stronger heterogeneity levels would therefore be of significant interest for further validation of the TBS method and has been identified as an important direction for future work. This study has been limited to 2D only. It may be mentioned here that the CBS method has already been tackled large 3D problems [17], [18]. We are planning to implement the same method or other variants to handle large problems, particularly 3D problems in the context of ultrasonics.

5. Conclusions

In this study, a detailed derivation for the TBS framework pertaining to biomedical ultrasound is presented. The pressure field for a linear array of point sources has been calculated. The propagating medium has been assumed to be absorbing, dispersive and heterogeneous. The developed CUDA C program, realizing the TBS formula and running on a workstation, took about 5 s to compute the pressure field (convergence reached after approximately 125 iterations). However, the runtime for the k-Wave program for the same workstation was approximately 560 s. A speed-up of more than two orders of magnitude relative to the time-domain k-Wave simulation is achieved. Furthermore, the results for the TBS and k-Wave approaches demonstrated excellent agreement, validating the proposed protocol. The TBS methodology turns out to be an appropriate computational framework for pressure field calculations in practice.

6. Acknowledgments

UM acknowledges financial support from the UGC-NFSC fellowship (Grant No. #F. 82-44/2020 (SA-III)). RKS gratefully recognizes funding support from ANRF (#CRG/2023/003278). BTC also acknowledges support from the UK Engineering and Physical Sciences Research Council (EPSRC), under grants EP/W029324/1 and EP/T014369/1.

References

[1] D. A. Cook et al., "Technology-enhanced simulation for health professions education: A systematic review and meta-analysis," *JAMA*, vol. 306, no. 9, pp. 978–988, 2011. DOI: 10.1001/jama.2011.1234.

[2] X. Wu, Y. Li, C. Su, P. Li, X. Wang, and W. Lin, "Ultrasound computed tomography based on full waveform inversion with source directivity calibration," *Ultrasonics*, vol. 132, p. 107 004, 2023. DOI: 10.1016/j.ultras.2023.107004.

[3] S. Bernard, V. Monteiller, D. Komatitsch, and P. Lasaygues, "Ultrasonic computed tomography based on full-waveform inversion for bone quantitative imaging," *Physics in Medicine & Biology*, vol. 62, no. 17, pp. 7011–7035, 2017. DOI: 10.1088/1361-6560/aa7e5a.

[4] N. McDannold, G. T. Clement, P. Black, F. Jolesz, and K. Hynynen, "Transcranial magnetic resonance imaging–guided focused ultrasound surgery of brain tumors: Initial findings in 3 patients," *Neurosurgery*, vol. 66, no. 2, pp. 323–

332, 2010. DOI: 10.1227/01.NEU.0000360379.95800.2F.

[5] C. R. Hill, J. C. Bamber, and G. R. ter Haar, *Physical Principles of Medical Ultrasonics*, 2nd ed. Chichester, U.K.: Wiley, 2004.

[6] T. L. Szabo, "Time domain wave equations for lossy media obeying a frequency power law," *The Journal of the Acoustical Society of America*, vol. 96, no. 1, pp. 491–500, 1994. DOI: 10.1121/1.410511.

[7] B. E. Treeby and B. T. Cox, "Modeling power law absorption and dispersion for acoustic propagation using the fractional laplacian," *The Journal of the Acoustical Society of America*, vol. 127, no. 5, pp. 2741–2748, 2010. DOI: 10.1121/1.3377056.

[8] M. Born, "Quantenmechanik der stoßvorgänge," *Zeitschrift für Physik*, vol. 38, no. 11–12, pp. 803–827, 1926.

[9] M. Osnabrugge, S. Leedumrongwatthanakun, and I. M. Vellekoop, "A convergent born series for solving the inhomogeneous helmholtz equation in arbitrarily large media," *Journal of Computational Physics*, vol. 322, pp. 113–124, 2016. DOI: 10.1016/j.jcp.2016.06.034.

[10] A. Kaushik, P. Yalavarthy, and R. K. Saha, "Convergent born series improves the accuracy of numerical solution of time-independent photoacoustic wave equation," *Journal of Modern Optics*, vol. 67, no. 9, pp. 849–855, 2020. DOI: 10.1080/09500340.2020.1728652.

[11] R. K. Saha, "Numerical solution to the time-independent inhomogeneous photoacoustic wave equation using the born series methods," *Journal of the Optical Society of America A*, vol. 37, no. 12, pp. 1907–1915, 2020. DOI: 10.1364/JOSAA.401398.

[12] U. Mandal et al., "Efficient implementations of a born series for computing photoacoustic field from a collection of erythrocytes," *Photoacoustics*, vol. 32, p. 100 724, 2023. DOI: 10.1016/j.pacs.2023.100724.

[13] U. Mandal, J. Singh, B. T. Cox, and R. K. Saha, "Graphics processing unit accelerated helmholtz equation solver in two dimensions using the traditional born series formulation for linear and nonlinear media in biomedical ultrasound," *The Journal of the Acoustical Society of America*, vol. 159, no. 3, pp. 1948–1962, Mar. 2026, ISSN: 0001-4966. DOI: 10.1121/10.0042817.

[14] P. M. Morse and H. Feshbach, *Methods of Theoretical Physics*. New York, NY, USA: McGraw-Hill, 1953.

[15] U. Mandal et al., "Efficient implementations of a born series for computing photoacoustic field from a collection of erythrocytes," *Photoacoustics*, vol. 43, p. 100 724, 2025.

[16] J. Blackmore, S. Shrivastava, J. Sallet, C. R. Butler, and R. O. Cleveland, "Ultrasound neuromodulation: A review of results, mechanisms and safety," *Ultrasound in medicine & biology*, vol. 45, no. 7, pp. 1509–1536, 2019.

[17] R. K. Saha, "Solving time-independent inhomogeneous optoacoustic wave equation numerically with a modified green's function approach," *Journal of the Acoustical Society of America*, vol. 149, no. 6, pp. 4039–4048, 2021. DOI: 10.1121/10.0005973.

[18] S. Mache and I. M. Vellekoop, "Domain decomposition of the modified born series approach for large-scale wave propagation simulations," *Journal of Computational Physics*, p. 114 619, 2025.